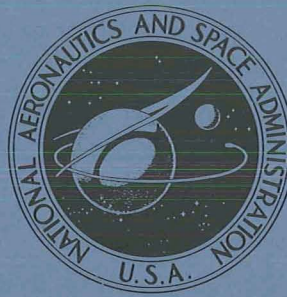


NASA TECHNICAL
MEMORANDUM



NASA TM X-1962

NASA TM X-1962

CASE FILE
COPY

NEUTRON AND GAMMA MEASUREMENTS
FOR THE NASA PLUM BROOK REACTOR
HB-6 BEAM HOLE INSERTION FACILITY

by Suzanne T. Weinstein and James A. Kish

Lewis Research Center

Cleveland, Ohio

1. Report No. NASA TM X-1962	2. Government Accession No.	3. Recipient's Catalog No.	
4. Title and Subtitle NEUTRON AND GAMMA MEASUREMENTS FOR THE NASA PLUM BROOK REACTOR HB-6 BEAM HOLE INSERTION FACILITY		5. Report Date February 1970	
		6. Performing Organization Code	
7. Author(s) Suzanne T. Weinstein and James A. Kish		8. Performing Organization Report No. E-5358	
9. Performing Organization Name and Address Lewis Research Center National Aeronautics and Space Administration Cleveland, Ohio 44135		10. Work Unit No. 120-27	
		11. Contract or Grant No.	
12. Sponsoring Agency Name and Address National Aeronautics and Space Administration Washington, D. C. 20546		13. Type of Report and Period Covered Technical Memorandum	
		14. Sponsoring Agency Code	
15. Supplementary Notes			
16. Abstract The fast and thermal neutron fluxes in the NASA Plum Brook Reactor HB-6 beam hole were measured using standard neutron activation techniques. The gamma ray exposure rate in the beam hole was measured with argon-filled ion chambers. The measurements were made as a function of position along the HB-6 beam. The fast neutron flux varied from $2.5 \pm 0.9 \times 10^9$ to $1.2 \pm 0.4 \times 10^7$ neutrons/(cm ²)(sec), the thermal neutron flux varied from $1.5 \pm 0.5 \times 10^9$ to $3.4 \pm 1.0 \times 10^6$ neutrons/(cm ²)(sec), and the gamma ray exposure rate varied from $1.4 \pm 0.3 \times 10^7$ to $1.2 \pm 0.2 \times 10^5$ R/hr. The effects of position across the beam face and of reactor shim rod bank height were also determined.			
17. Key Words (Suggested by Author(s)) Reactor flux Thermal neutron flux Fast neutron flux Gamma exposure rate		18. Distribution Statement Unclassified - unlimited	
19. Security Classif. (of this report) Unclassified	20. Security Classif. (of this page) Unclassified	21. No. of Pages 19	22. Price* \$3.00

*For sale by the Clearinghouse for Federal Scientific and Technical Information
Springfield, Virginia 22151

NEUTRON AND GAMMA MEASUREMENTS FOR THE NASA PLUM

BROOK REACTOR HB-6 BEAM HOLE INSERTION FACILITY

by Suzanne T. Weinstein and James A. Kish

Lewis Research Center

SUMMARY

The fast and thermal neutron fluxes and the gamma ray exposure rate were measured in the HB-6 beam hole insertion facility of the NASA Plum Brook Reactor. The measurements were made as a function of position along the HB-6 beam, of position across the beam face, and of reactor shim-rod bank height. The fast and thermal neutron attenuation factors were measured for the test cavity attenuator shields. The data were normalized to a reactor operating power of 40 megawatts.

The fast neutron flux was measured by the neutron activation of sulfur and nickel. The fast neutron flux (energies greater than 2.9 MeV) varies along the beam from $2.5 \pm 0.9 \times 10^9$ at full forward to $1.2 \pm 0.4 \times 10^7$ neutrons per square centimeter-second in the test cavity. The thermal neutron flux was measured by the neutron activation of dysprosium and cobalt. The thermal flux varies along the beam from $1.5 \pm 0.5 \times 10^9$ to $3.4 \pm 1.0 \times 10^6$ neutrons per square centimeter-second. The test cavity attenuator shields provide fast neutrons attenuation up to a factor of 10 and thermal neutron attenuation of over a factor of 100.

The gamma ray exposure rate was measured with stainless steel, argon-filled ion chambers. The exposure rate varies along the beam from $1.4 \pm 0.3 \times 10^7$ roentgens per hour at the full forward position to $1.2 \pm 0.2 \times 10^5$ roentgens per hour in the test cavity.

INTRODUCTION

Semiconductor components intended for use in nuclear space power generating systems must be capable of operating reliably in a reactor environment. An insertion facility was constructed in the HB-6 beam hole of the NASA Plum Brook reactor to provide a facility for semiconductor components testing in a mixed neutron and gamma ray

environment. A knowledge of the fast neutron flux and the gamma ray exposure rate in the insertion facility is needed for the proper assessment of permanent and transient radiation damage effects. In addition, data on the thermal neutron flux are needed for calculation of the neutron activation of test specimens.

The fluxes and exposure rate are affected primarily by position along the HB-6 beam and the presence of fast neutron attenuator shields in the test cavity of the facility. Secondary factors include reactor power level, reactor shim-rod bank height, and vertical and horizontal position across the beam face. The fast neutron flux was measured with sulfur pellets and nickel wires. Dysprosium and cobalt foils were used for the thermal neutron flux measurements. The gamma ray exposure rate was measured with stainless steel, argon-filled ion chambers.

FACILITY DESCRIPTION

The HB-6 beam hole is an air-filled thimble approximately 3.7 meters long. The closed end (38 cm in diam) adjoins the reactor beryllium reflector and is cadmium covered and water cooled. The opposite end (46 cm in diam) opens into a test cavity which is surrounded by steel-jacketed, borated-paraffin shielding. The total facility length, including the test cavity, is 4.2 meters (see fig. 1). The insertion facility is a modification of a prior facility (see ref. 1) and has been designed to provide a greater range of fluxes. The insertion system basically consists of a chain-driven carriage mounted on rails, with a total drive length of 3.9 meters from the test cavity position to full-forward. Test specimens up to 28 centimeters in diameter and 60 centimeters long can be inserted to the full forward position. Larger specimens up to 38 centimeters in diameter can be accommodated in the test cavity. An aluminum plate containing neutron and/or gamma dosimeters can be installed on and removed from the carriage during reactor operation through a slot in the shielding. The distance attenuation was expected to provide about two orders of magnitude variation in the fast neutron flux. To provide additional fast neutron attenuation, up to a factor of 10, a series of three test cavity attenuator shields was designed. Each shield consists of a borated-polyethylene sandwiched between aluminum plates, on which provision was made for dosimeter mounting. Figure 2 shows the attenuator shields installed in the test cavity and the specimen plate position.

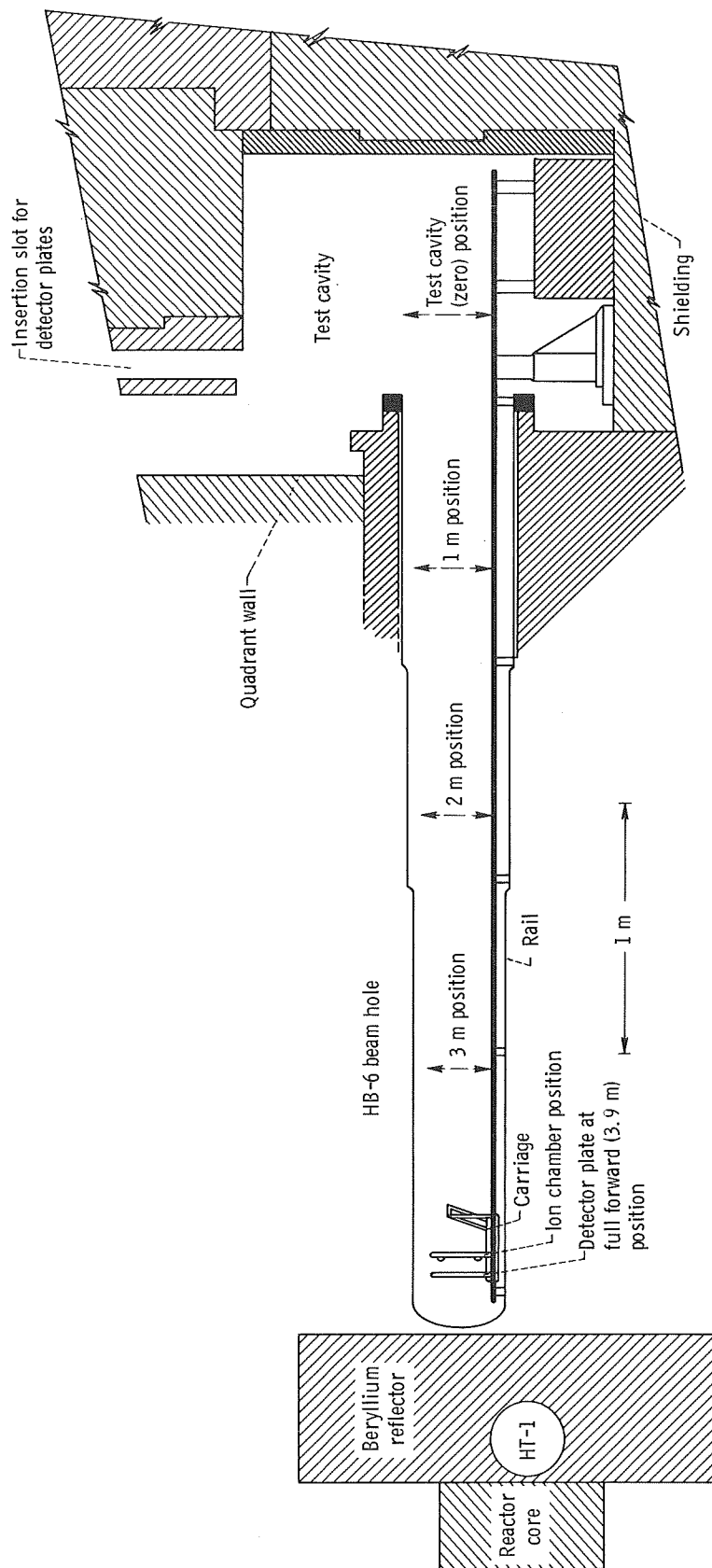


Figure 1. - HB-6 beam hole insertion facility. (Indicated positions are for detector plate at front of carriage).

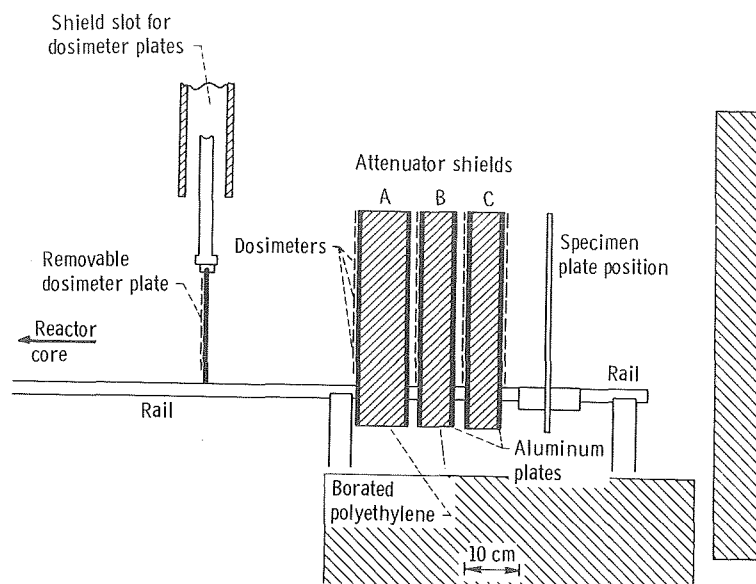


Figure 2. - Neutron attenuator shields and specimen plate configuration in test cavity.

NEUTRON FLUX MEASUREMENTS

The fast and thermal neutron fluxes in the HB-6 Insertion Facility were measured as a function of position along the HB-6 beam. The variations of flux with reactor shim-rod bank height and with vertical and horizontal position across the beam face were also determined. The fast and thermal neutron attenuation factors obtained with the test cavity attenuator shields were measured.

Experimental Procedures

All neutron flux measurements were made using standard neutron activation techniques. A known detector mass is exposed to a neutron beam for a specific period of time; the neutron-induced activity from a specific reaction is measured; and the standard activation and decay equations are used to calculate the neutron flux (see the appendix). Table I lists the detectors used, the reaction of interest, the reaction product half-life, and the neutron cross section (with references) used in calculating the flux.

The "in-hole" flux measurements were made at the test cavity (zero) position; at 1, 2, and 3 meters into the beam hole; and at the full-forward (3.9-m) position (see fig. 1). The neutron detectors were taped to an aluminum detector plate at the positions

TABLE I. - FAST AND THERMAL NEUTRON FLUX DETECTORS

Neutron flux	Detector			Reaction	Reaction product	Half-life	Effective cross section, barn (a)	Effective neutron energy	Reference
	Material	Diameter, cm	Thickness, cm						
Fast	Sulfur	1.27	0.47	$S^{32}(n, p)$	P^{32}	14.3 days	0.30 ± 0.023	2.9 MeV	2
	Nickel	1.27	0.08	$Ni^{58}(n, p)$	Co^{58}	71.3 days	0.42 ± 0.043	5.0 MeV	2
Thermal	Dysprosium	0.62	0.025	$Dy^{164}(n, \gamma)$	Dy^{165}	2.32 hr	(b)	0.025 eV	---
	Cobalt	0.62	0.025	$Co^{59}(n, \gamma)$	Co^{60}	5.27 yr	37.2 ± 0.6	0.025 eV	3

^aEffective fast neutron cross sections are defined in terms of the unmoderated fission neutron spectrum.

^bDysprosium foils were calibrated against standard gold foils at PBRF (see ref. 4).

across the beam face shown in figure 3. A detector plate for each exposure was inserted through the shielding and placed on the carriage. The carriage was moved to a measurement position for a predetermined exposure period and then withdrawn for removal of that plate and insertion of the next. Sulfur pellets and nickel wires were used to measure the fast neutron flux. Sulfur was used at all positions except full forward, where the ambient temperature was too high for sulfur. Nickel was substituted at the full-forward position and was also used at 3 meters for comparison. Dysprosium foils were used for all thermal neutron flux measurements in hole. Flux measurements at all five in-hole positions were repeated periodically throughout one full reactor cycle (nominal 20 days) to determine the effect of reactor shim-rod bank height. The test

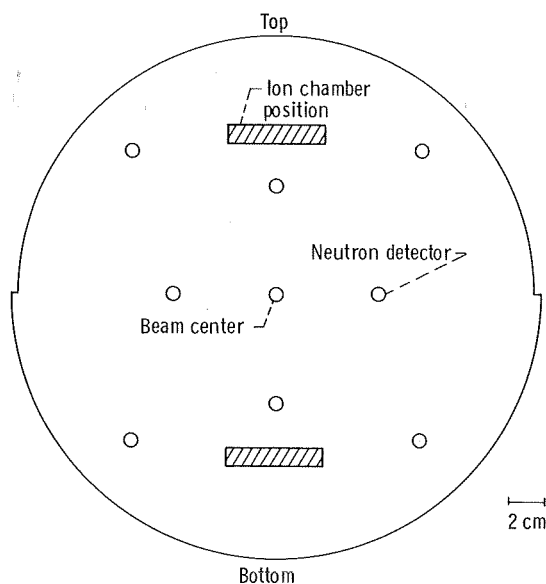


Figure 3. - Neutron detector and ion chamber positions for in-hole measurements.

cavity neutron attenuator shields were not installed during this reactor cycle.

The fast and thermal neutron attenuation factors for the test cavity attenuator shields were measured during the following reactor cycle. Detectors were mounted in front of, at two inner positions, and behind the attenuators (fig. 2) at the positions across the beam face shown in figure 4. Sulfur pellets were again used for the fast flux. Because of activity saturation, cobalt foils were substituted for the dysprosium for thermal flux measurements. The exposure period covered the entire reactor cycle (abbreviated to 7 days) since the test cavity cannot be opened while the reactor is at power.

Following exposure, the detectors were removed from the plates and the neutron-induced activity was measured. The sulfur and dysprosium activities were measured with a calibrated 2π gas-flow proportional beta counter. The nickel and cobalt activities were measured with a calibrated sodium iodide gamma ray spectrometer. Using the equations of the appendix, the neutron fluxes were then computer-calculated from these activities and normalized to a reactor power level of 40 megawatts.

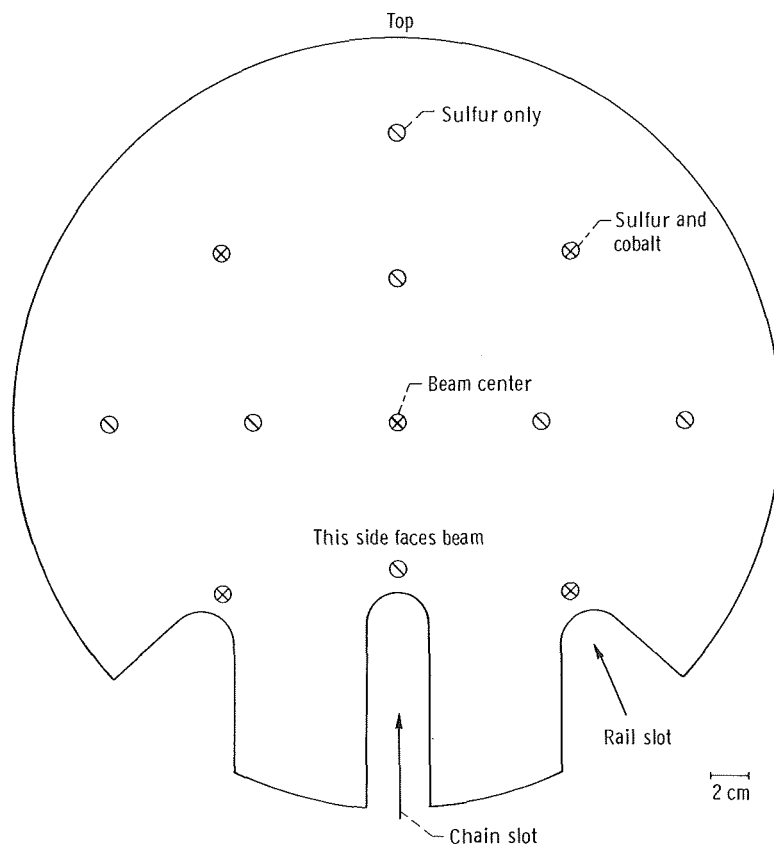


Figure 4. - Detector positions for test cavity attenuator shields.

Results and Discussion

The average (over the plate) fast and thermal neutron fluxes at midcycle (shim rods at 55 cm) are shown in figure 5 as a function of position along the HB-6 beam. The average fast neutron flux (energies greater than 2.9 MeV) at reactor midcycle varies along the HB-6 beam by about a factor of 200: from $2.5 \pm 0.9 \times 10^9$ neutrons per square centimeter-second at the full-forward (3.9-m) position to $1.2 \pm 0.4 \times 10^7$ neutrons per square centimeter-second at the test cavity (zero) position. The average thermal neutron flux at midcycle (shim rods at 55 cm) varies along the beam by a factor of about 400 from $1.5 \pm 0.5 \times 10^9$ neutrons per square centimeter-second at full forward to $3.4 \pm 1.0 \times 10^6$ neutrons per square centimeter-second at the test cavity.

The secondary factors affecting the neutron fluxes are reactor shim rod bank height and position across the beam face. The core power density maximum moves from the bottom to the top of the reactor core as the shim rod bank is raised from about 40 to 70 centimeters during the course of a reactor cycle. The fluxes also vary across

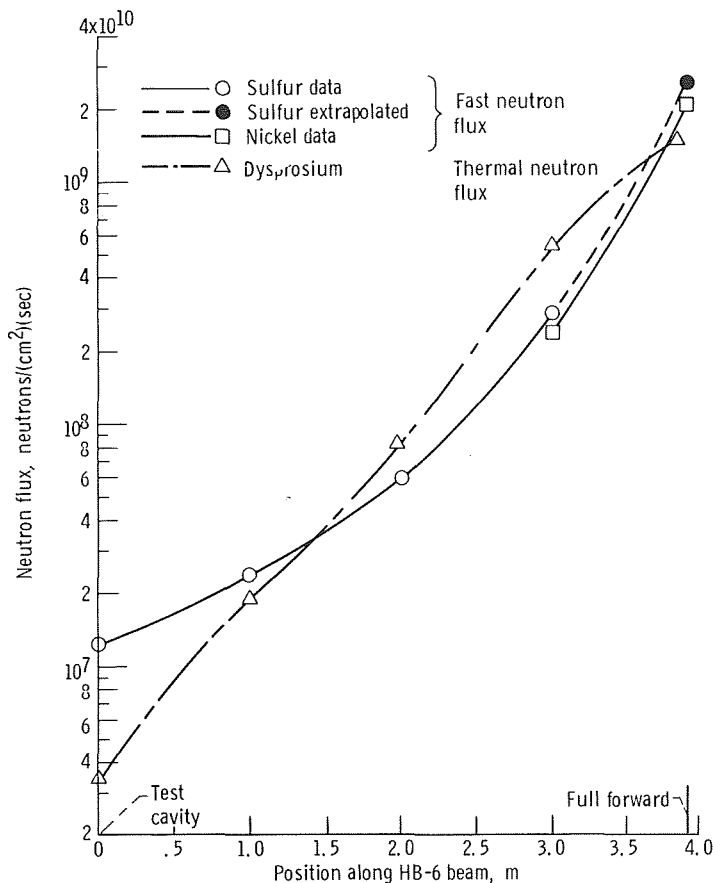


Figure 5. - Average fast and thermal neutron flux at midcycle as function of position along HB-6 beam. (Shim rod bank height equals 55 cm.)

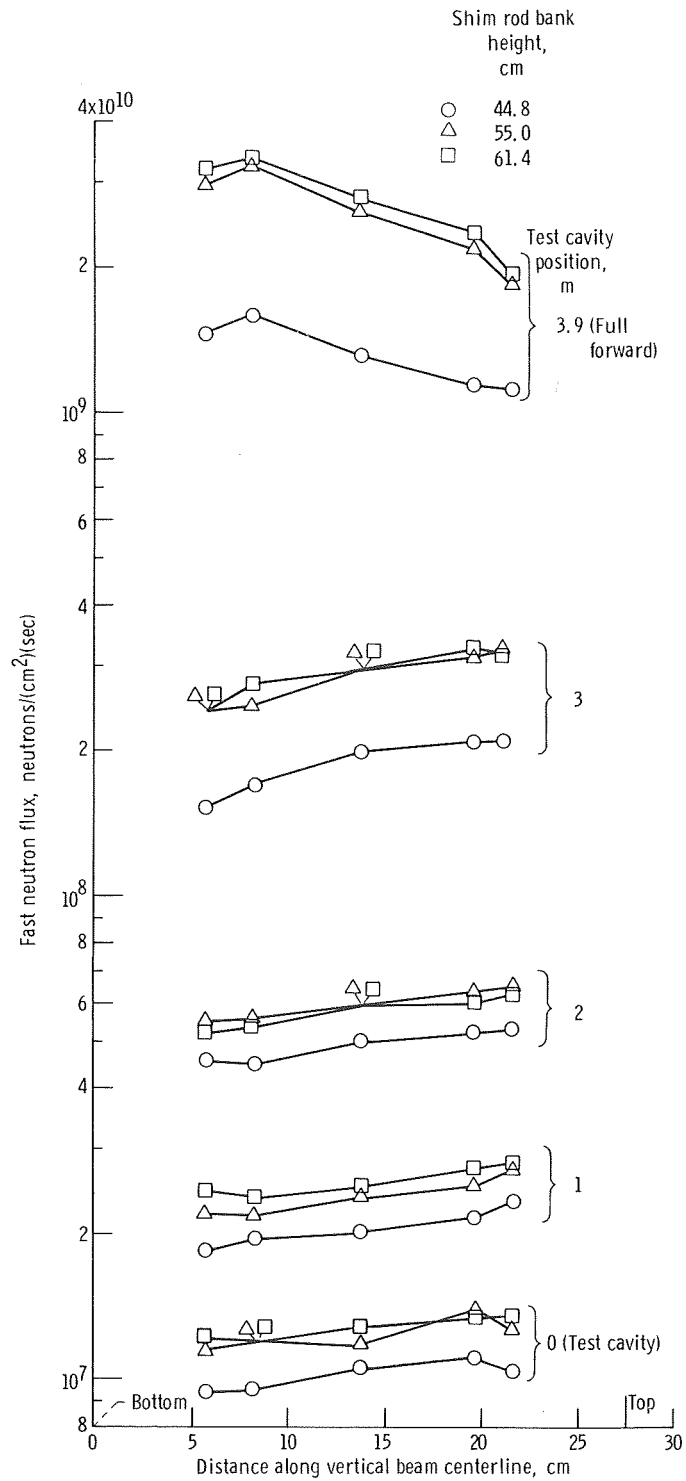


Figure 6. - Fast neutron flux as function of distance along vertical beam centerline for three shim rod bank heights.

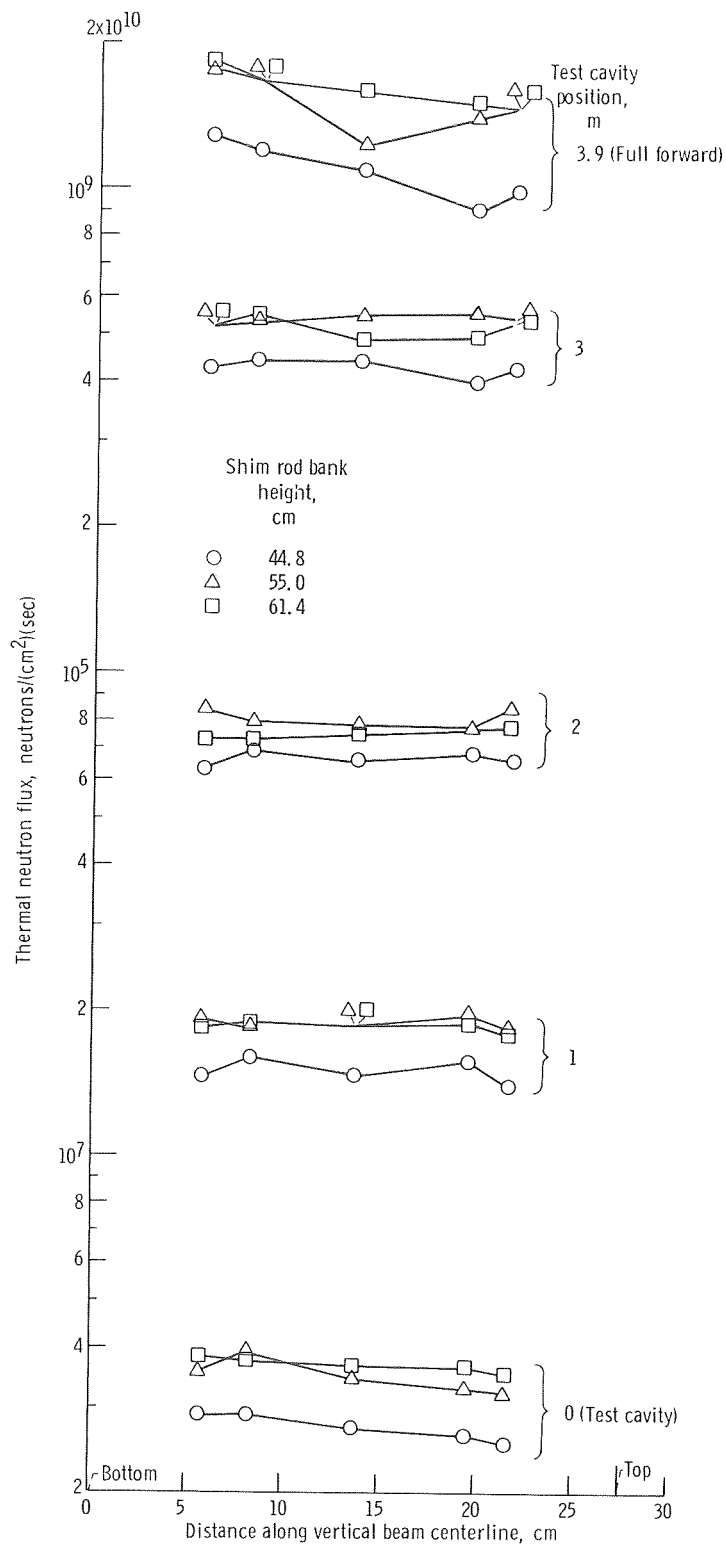


Figure 7. - Thermal neutron flux as function of distance along vertical beam centerline for three shim rod bank heights.

the beam face due to the location of the HB-6 beam duct and to the presence of other experimental facilities, particularly HT-1 (see fig. 1). The average fast and thermal fluxes as a function of position along the vertical beam centerline at all five measurement positions along the beam are shown in figures 6 and 7 for three shim rod bank heights. Both the fast and thermal fluxes are nearly symmetrical about the vertical centerline and were averaged to obtain the fluxes on the centerline. The fluxes increase rapidly with increased bank height at the start of the cycle and then nearly saturate at about midcycle. This effect is due to the combination of the upward movement of the core power maximum and the presence of the HT-1 beam duct. Both the fast and thermal neutron fluxes at the full forward position are greater at the bottom of the beam than at the top. At the other measurement positions (0, 1, 2, and 3 m), the fast flux is greater at the top and the thermal flux is nearly uniform across the beam. These distributions do not vary greatly with the shim rod bank height and are produced by the amount and type of materials lying along the neutron lines-of-sight.

The average (over the plate) fast and thermal neutron attenuation factors obtained with the test cavity attenuator shields are shown in figure 8. Various combinations of the three shields will produce test cavity fast neutron flux attenuation by factors of about 2, 3, 5, and 10. Over a hundredfold thermal neutron flux attenuation was produced by the three shields. The presence of the attenuators does not greatly alter the flux distributions across the face of the beam.

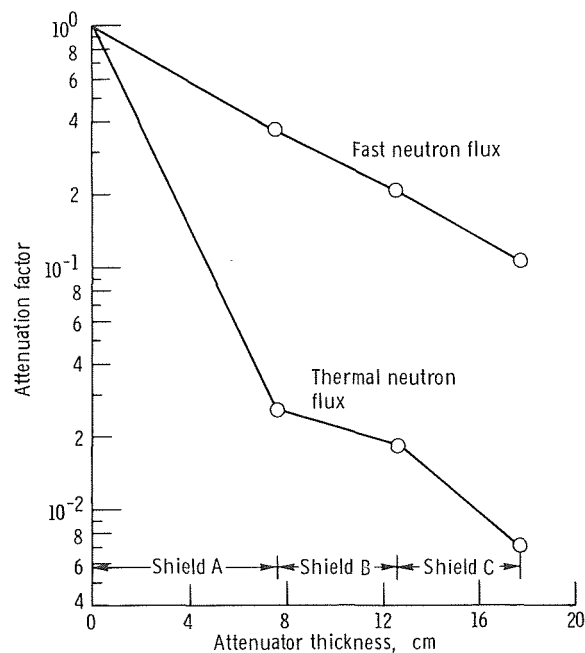


Figure 8. - Average fast and thermal neutron attenuation factors for test cavity attenuator shields.

Measurements of relative neutron flux by means of activation techniques can be made quite accurately. The error source for relative measurements are experimental: exposure time and position, detector weight and purity, and activity counting. The net experimental error in the relative fluxes, and in the fast neutron attenuation factors for the test cavity shields are 11 percent or less. The thermal neutron attenuation factor error is about 11 percent. However, absolute neutron flux measurements are far less accurate. The neutron cross section and the threshold energy for fast neutrons are large error sources in calculating the neutron flux from detector activities. However, the major source of uncertainty is the fast neutron spectrum. Reference 5 discusses this problem in detail for the HB-6 facility. The net absolute flux errors at the 90 percent confidence level are about 35 and 15 percent for fast and thermal neutron fluxes, respectively.

GAMMA EXPOSURE RATE MEASUREMENTS

The gamma ray exposure rates were measured as a function of position along the HB-6 beam. Measurements were made at two positions (top and bottom) along the vertical beam centerline. The variation of exposure rate with reactor shim rod bank height was also determined.

Experimental Procedures

The gamma exposure rates were measured with two stainless steel, argon-filled ion chambers which were 6.4 centimeters long and 0.64 centimeter in outside diameter. The ion chambers were mounted on the test carriage, near the top and the bottom of the beam, approximately 8 centimeters behind the neutron detector plate position as shown in figure 1. The neutron detector plate was not in position on the carriage during the gamma measurements. The positions of the ion chambers relative to the neutron detectors is shown in figure 3. The chambers were calibrated prior to use in the spent-fuel-element gamma facility at the Plum Brook Reactor. The current-to-exposure rate conversion factor for both ion chambers is $1.1 \pm 0.2 \times 10^{13}$ roentgens per hour per ampere.

The exposure rate was measured at the same test carriage positions along the HB-6 beam as the neutron fluxes: test cavity, 1, 2, and 3 meters, and full forward. Measurements were also made at 2.5 and 3.5 meters. All measurements were made four times during a 20-day reactor cycle to determine the effects of shim-rod bank height on the exposure rates. The effect of the test cavity neutron attenuator shields on the gamma ex-

posure rate was not measured. Exposure rates were normalized to a reactor power level of 40 megawatts.

Results and Discussion

Figure 9 shows the gamma exposure rate at midcycle for both chamber positions as a function of distance along the HB-6 beam. The average gamma ray exposure rate at reactor midcycle (shim rods at 56 cm) varies along the beam by a factor of about 100

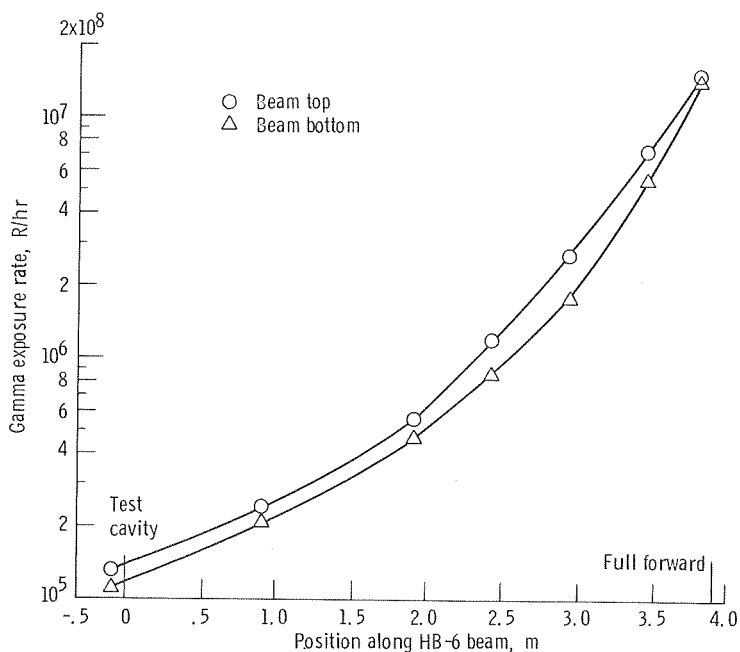


Figure 9. - Gamma exposure rate at midcycle as function of position along beam for both ion chambers. (Shimrod bank height equals 56.4 cm.)

from $1.4 \pm 0.3 \times 10^7$ roentgens per hour at the full-forward position to $1.2 \pm 0.2 \times 10^5$ roentgens per hour in the test cavity. The exposure rate rises smoothly with distance into the beam hole with the rate consistently somewhat higher at the top of the beam.

The effects of reactor shim rod bank height and position across the beam face can be seen in figure 10. The exposure rate increases exponentially with bank height at all positions, but percentage increase is least at the full-forward position and greatest in the test cavity. This is probably the combined result of core power maximum movement and scattering in the beam duct walls. The top and bottom exposure rates are nearly equal at full forward, diverge rapidly to a maximum spread at about 3 meters,

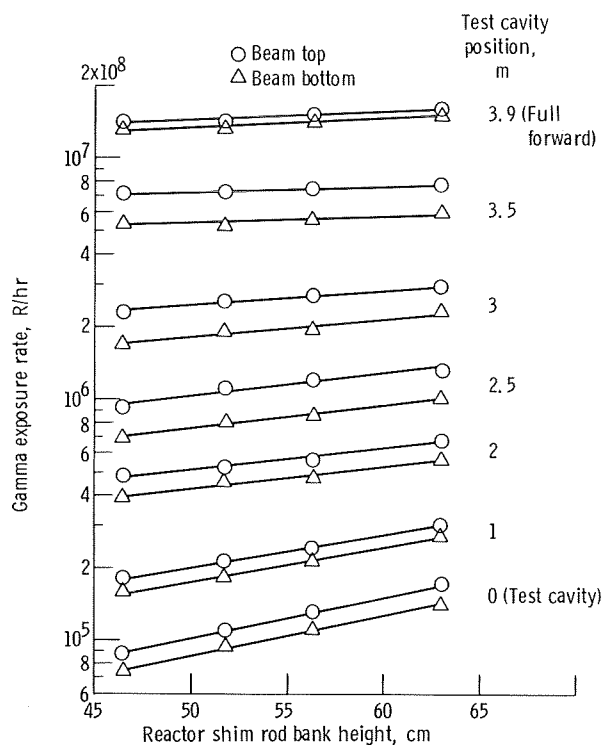


Figure 10. - Gamma exposure rate as function of shim rod bank ion chambers.

and slowly converge again toward the test cavity. The cause of this variation in the top-to-bottom ratio is not readily identifiable.

The error in the relative exposure rates is about ± 5 percent, due to position and metering errors. The absolute gamma exposure rates are in error by about ± 20 percent at the 90 percent confidence level.

SUMMARY OF RESULTS

The fast and thermal neutron fluxes and the gamma ray dose rate were measured in the HB-6 beam hole insertion facility of the Plum Brook Reactor. The following results were obtained:

1. The average fast neutron flux (energies greater than 2.9 MeV) at reactor mid-cycle varies along the beam by about a factor of 200: from $2.5 \pm 0.9 \times 10^9$ to $1.2 \pm 0.4 \times 10^7$ neutrons per square centimeter-second.

2. The average thermal neutron flux at reactor midcycle varies along the beam by a factor of about 400: from $1.5 \pm 0.5 \times 10^9$ to $3.4 \pm 1.0 \times 10^6$ neutrons per square centimeter-second.

3. The fast and thermal neutron fluxes increase with reactor shim rod bank height during the first part of the reactor cycle and then nearly saturate at about midcycle (shim rod at 55 cm). The amount of flux increase varies with position along the beam.

4. The fast and thermal neutron fluxes are nearly symmetrical about the vertical beam centerline. Both fast and thermal fluxes are greatest at the bottom of the beam at the full-forward position. The fast flux is greater at the top of the beam and the thermal flux is nearly constant at all other measurement positions along the beam.

5. The test cavity attenuator shields provide fast neutron attenuation up to a factor of 10 and thermal neutron attenuation of over a factor of 100.

6. The average gamma ray exposure rate at reactor midcycle varies along the beam by a factor of about 100 from $1.4 \pm 0.3 \times 10^7$ roentgens per hour at full forward to $1.2 \pm 0.2 \times 10^5$ roentgens per hour in the test cavity.

7. The gamma ray exposure rate increases exponentially with increasing reactor shim rod bank height. The percentage increase varies with position along the HB-6 beam.

8. The gamma ray exposure rate is consistently somewhat higher at the top of the beam. The ratio of the top-to-bottom exposure rate is a function of position along the beam.

Lewis Research Center,

National Aeronautics and Space Administration,

Cleveland, Ohio, November 6, 1969

120-27.

APPENDIX - SUMMARY OF NEUTRON FLUX MEASUREMENTS BY RADIOACTIVATION

Fast and thermal neutron flux measurements by radioactivation are in general the same. Specific technique variations will be discussed separately in this appendix. Basically, a known number of atoms of a particular element isotope are exposed to a neutron flux for a measured period of time and neutron-induced activity is measured. The "saturated activity" and the neutron flux are then calculated (see ref. 2).

The "saturated activity" is the induced activity corresponding to the steady state in which the rate of production by neutron absorption is equal to the rate of loss by radioactive decay. When the counting (measurement) period is short compared to the half-life of the radioactive nuclide, the saturated activity (in disintegrations/atom) is given by

$$A = \frac{CR}{\epsilon W \rho_A \left(1 - e^{-\lambda t_i}\right) e^{-\lambda t_d}} \quad (1)$$

where

- CR background-corrected count-rate, disintegrations/sec
- ϵ counter efficiency, number of counts observed/disintegration
- W detector weight, g
- ρ_A number of target-isotope atoms per gram of detector material
- λ product-isotope decay constant, $\ln 2$ /product half-life
- t_i exposure time
- t_d decay time (from end of exposure to start of counting)

The neutron flux is related to the saturated activity by

$$A = \int_0^{\infty} \sigma(E) \varphi(E) dE \quad (2)$$

where

- $\sigma(E)$ activation cross section at energy E
- $\varphi(E)$ differential neutron flux, i. e., $\varphi(E)dE$ is neutron flux at energies between E and E + dE

Thermal (2200 m/sec) Neutron Flux

In a pure thermal neutron flux, where the most probable neutron velocity is 2200 meters per second, equation (2) reduces to

$$\Phi_{th(pure)} = \frac{A}{\sigma_{th}} \quad (3)$$

where σ_{th} is the activation cross section for thermal (2200 m/sec) neutrons. Since neutrons of all energies are usually present, the saturated activity must be corrected for the nonthermal contribution to the induced activity. This requires the simultaneous exposure of bare and cadmium-covered detectors. Cadmium screens out effectively all thermal neutrons, so that the covered detector activity yields the nonthermal neutron activity contribution. In addition, flux depression due to the presence of the detector must be corrected for. The net correction factor to be applied to the saturated, bare activity (eq. (1)) is

$$K = \frac{\left(1 - \frac{F_{Cd}}{R_{Cd}}\right)}{F_{th}} \quad (4)$$

where

F_{Cd} epithermal flux depression factor due to cadmium

R_{Cd} ratio of bare to cadmium-covered activities

F_{th} thermal flux depression factor due to detector

The actual thermal neutron flux in a mixed thermal-epithermal field (from eq. (3)) is given by

$$\Phi_{th(mixed)} = \frac{KA}{\sigma_{th}} \quad (5)$$

Fast Neutron Flux

The fast neutron flux is determined by threshold detectors which measure the integral flux of neutrons having energies greater than some threshold energy. The acti-

vation cross section for an ideal detector is a step function; that is, it is zero for neutrons with energies below the threshold energy E_i and is a constant σ_{E_i} for neutron energies above E_i . In this case, equation (2) can be written as

$$A = \sigma_{E_i} \int_{E_i}^{\infty} \varphi(E) dE \quad (6)$$

However, the cross section as a function of energy for a real detector does not exhibit step-function characteristics. The rapid increase in cross section is not infinitely steep, requiring a somewhat arbitrary selection of the threshold energy; and the cross section does not reach a constant value, which would require the use of an averaging process:

$$\sigma_{E_i} = \frac{\int_0^{\infty} \sigma(E) \eta(E) dE}{\int_{E_i}^{\infty} \eta(E) dE} \quad (7)$$

where $\eta(E)$ is a differential neutron spectrum, which is usually chosen as the unmoderated fission neutron spectrum.

The integral fast flux for fission neutrons having energies greater than E_i is then

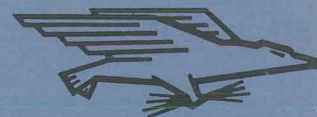
$$\Phi_f = \frac{A}{\sigma_{E_i}} \quad (8)$$

where A is the saturated activity calculated from equation (1). The integral fast flux can be corrected for deviations of the actual spectrum from a fission spectrum, provided the actual spectrum is well known. Generally, the actual spectrum is not known and the lack of this correction factor is the dominant source of error in fast neutron flux measurements.

REFERENCES

1. Smith, John R.; Kroeger, Erich W.; Asadourina, Armen S.; and Spagnuolo, Adolph C.: Fast-Neutron Beam Irradiation Facility in the NASA Plum Brook Test Reactor. NASA TM X-1374, 1967.

2. Anon. : Measuring Neutron Flux by Radioactivation Techniques. Designation: E261-65T, ASTM, 1965.
3. Goldberg, Murrey D. ; et al: Neutron Cross Sections. Rep. BNL-325, 2nd ed. , Suppl. 2, vol. 2, pts. A, B, C, Brookhaven Nat. Lab. , 1966.
4. Anon. : Measuring Thermal Neutron Flux by Radioactivation Techniques. Designation: E262-65T, ASTM, 1965.
5. Bozek, John M. ; and Godlewski, Michael P. : Experimental Determination of Neutron Fluxes in Plum Brook Reactor HB-6 Facility with Use of Sulfur Pellets and Gold Foils. NASA TM X-1497, 1968.



POSTMASTER: If Undeliverable (Section 158
Postal Manual) Do Not Return

"The aeronautical and space activities of the United States shall be conducted so as to contribute . . . to the expansion of human knowledge of phenomena in the atmosphere and space. The Administration shall provide for the widest practicable and appropriate dissemination of information concerning its activities and the results thereof."

— NATIONAL AERONAUTICS AND SPACE ACT OF 1958

NASA SCIENTIFIC AND TECHNICAL PUBLICATIONS

TECHNICAL REPORTS: Scientific and technical information considered important, complete, and a lasting contribution to existing knowledge.

TECHNICAL NOTES: Information less broad in scope but nevertheless of importance as a contribution to existing knowledge.

TECHNICAL MEMORANDUMS: Information receiving limited distribution because of preliminary data, security classification, or other reasons.

CONTRACTOR REPORTS: Scientific and technical information generated under a NASA contract or grant and considered an important contribution to existing knowledge.

TECHNICAL TRANSLATIONS: Information published in a foreign language considered to merit NASA distribution in English.

SPECIAL PUBLICATIONS: Information derived from or of value to NASA activities. Publications include conference proceedings, monographs, data compilations, handbooks, sourcebooks, and special bibliographies.

TECHNOLOGY UTILIZATION PUBLICATIONS: Information on technology used by NASA that may be of particular interest in commercial and other non-aerospace applications. Publications include Tech Briefs, Technology Utilization Reports and Notes, and Technology Surveys.

Details on the availability of these publications may be obtained from:

SCIENTIFIC AND TECHNICAL INFORMATION DIVISION
NATIONAL AERONAUTICS AND SPACE ADMINISTRATION
Washington, D.C. 20546